



ELSEVIER

Contents lists available at ScienceDirect

## ISA Transactions

journal homepage: [www.elsevier.com/locate/isatrans](http://www.elsevier.com/locate/isatrans)

## Research Article

# Stabilization loop of a two axes gimbal system using self-tuning PID type fuzzy controller



Maher Mahmoud Abdo<sup>a,\*</sup>, Ahmad Reza Vali<sup>a</sup>, Ali Reza Toloei<sup>b</sup>, Mohammad Reza Arvan<sup>a</sup>

<sup>a</sup> Malek Ashtat University of Technology, Department of Electrical Engineering, Lavizan, Tehran, Iran

<sup>b</sup> Shahid Behehti University, Department of Aerospace, Tehran, Iran

## ARTICLE INFO

## Article history:

Received 29 June 2013

Received in revised form

17 November 2013

Accepted 3 December 2013

Available online 22 January 2014

This paper was recommended for

publication by A.B. Rad

## Keywords:

Gimbal system

Line of sight

Rate gyro

Inertia stabilization system

Stabilization loop

## ABSTRACT

The application of inertial stabilization system is to stabilize the sensor's line of sight toward a target by isolating the sensor from the disturbances induced by the operating environment. The aim of this paper is to present two axes gimbal system. The gimbals torque relationships are derived using Lagrange equation considering the base angular motion and dynamic mass unbalance. The stabilization loops are constructed with cross coupling unit utilizing proposed fuzzy PID type controller. The overall control system is simulated and validated using MATLAB. Then, the performance of proposed controller is evaluated comparing with conventional PI controller in terms of transient response analysis and quantitative study of error analysis. The simulation results obtained in different conditions prove the efficiency of the proposed fuzzy controller which offers a better response than the classical one, and improves further the transient and steady-state performance.

© 2013 ISA. Published by Elsevier Ltd. All rights reserved.

## 1. Introduction

The optical equipments (such as IR, radar, laser, and television) have found a wide use in many important applications, for example image processing, guided missiles, tracking systems, and navigation systems. In such systems, the optical sensor axis must be accurately pointed from a movable base to a fixed or moving target. Therefore, the sensor's line of sight (LOS) must be strictly controlled. In such an environment where the equipment is typically mounted on a movable platform, maintaining sensor orientation toward a target is a serious challenge. An Inertial Stabilization Platform (ISP) is an appropriate way that can solve this challenge [1]. Usually, two axes gimbal system is used to provide stabilization to the sensor while different disturbances affect it. The most important disturbance sources are the base angular motion, the dynamics of gimbal system, and the gimbal mass unbalance. It is therefore necessary to capture all the dynamics of the plant and express the plant in analytical form before the design of gimbal assembly is taken up [2]. The system performance depends heavily on the accuracy of plant modelling. A typical plant for such problems consists of an electro-mechanical gimbal assembly having angular freedom in one, two or three axes

and one or more electro-optical sensors [3]. The control of such LOS inertia stabilization systems is not a simple problem because of cross-couplings between the different channels. In addition, such systems are usually required to maintain stable operation and guarantee accurate pointing and tracking for the target even when there are changes in the system dynamics and operational conditions. The mathematical model and the control system of two axes gimbal system have been studied in many researches. Concerning the mathematical model, several derivations have been proposed using different assumptions. In [4], the kinematics and geometrical coupling relationships for two degree of freedom gimbal assembly have been obtained for a simplified case when each gimbal is balanced and the gimballed elements bodies are suspended about principal axes. [5] presented the equations of motion for two axes gimbal configuration, assuming that gimbals are rigid bodies and have no mass unbalance. In [5], Ekstrand has shown that inertia disturbances can be eliminated by certain inertia symmetry conditions, and certain choices of inertia parameters can eliminate the inertia cross couplings between gimbal system channels. A single degree of freedom gimbal operating in a complex vibration environment has been presented by Daniel in [6]. He illustrated how the vibrations excite both static and dynamic unbalance disturbance torques that can be eliminated by statically and dynamically balancing the gimbal which is regarded costly and time consuming [6]. In [7], the motion equations have been derived assuming that gimbals have no dynamic mass imbalance and without highlighting the effects of base angular velocities.

\* Corresponding author. Tel.: +98 937 750 4893.

E-mail addresses: [maherabdo74@yahoo.com](mailto:maherabdo74@yahoo.com) (M.M. Abdo), [ar.vali@aut.ac.ir](mailto:ar.vali@aut.ac.ir) (A.R. Vali), [toloei@sbu.ac.ir](mailto:toloei@sbu.ac.ir) (A.R. Toloei), [arvan@mut.ac.ir](mailto:arvan@mut.ac.ir) (M.R. Arvan).

In [8], a two axes gimbal mechanism was introduced and just the modelling of azimuth axis was focused while the elevation angle was kept fixed and cross moments of inertia were taken to be zero. In both [5,9], the dynamical model of elevation and azimuth gimbals have been derived on the assumption that gimbals mass distribution is symmetrical so the products of inertia were neglected and the model was simplified. It must be mentioned, that most of these researches considered that the elevation and azimuth channels are identical so that one axis was simulated and tested. Therefore, the cross coupling, which is caused by base angular motion and the properties of gimbal system dynamics, was ignored. Also, it was supposed that gimbals mass distribution is symmetrical so the gimbals have not dynamic unbalance. In addition, Newton's law has been utilized to derive the mathematical model. On the other hand, the control system of two axes gimbal configuration has been constructed using different control approaches. In [7], a proxy-based sliding mode has been applied on two axes gimbal system; also [10] proposed the sliding mode control under the assumption of uncoupled identical elevation and azimuth channels. In [11], modern synthesis tools such as linear quadratic regulator (LQR) or linear quadratic Gaussian with loop transfer recovery (LQG/LTR) control for a wideband controller have also been used in the line of sight stabilization for mobile land vehicle. Also, [12] presented a linear quadratic Gaussian (LQG) algorithm for estimating and compensating in real time a particular class of disturbances. Besides conventional control methods, some advance control techniques such as robust control [13], variable structure control (VSC) [14], and  $H_\infty$  control methodology [15] were also applied in LOS inertia stabilization systems. However, a majority of these algorithms were complex and difficult to be realized. In recent years, the fuzzy control technology has been developed successfully. It improves the control system performance, and has the good adaptability for the system with non-linear mathematical model and uncertain factors [16,17]. Unlike the conventional control, the fuzzy logic control usually does not need the accurate mathematical model of the process which must be controlled and therefore fuzzy logic is considered one of the best solves for wide section of stubborn and challenging control problems [18,19]. There are two types of fuzzy logic-based controllers; Takagi Sugeno (T-S) based and Mamdani based. In literature, it can be found that almost all nonlinear dynamical systems can be represented by Takagi Sugeno fuzzy models to high degree of precision. In fact, it is proved that Takagi-Sugeno fuzzy models are universal approximators of any smooth nonlinear system [20]. When the fuzzy logic system is incorporated into adaptive control scheme, a stable fuzzy adaptive controller is obtained to be used in complex environments that impose perturbations on plant parameters. In such environments, this controller is used online to modify and adjust the control parameters automatically [17]. Basically, the adaptive fuzzy controllers have been developed for unknown SISO and MIMO nonlinear systems but they are limited only to nonlinear systems whose states can be measured [21]. A fuzzy control system was implemented in [22] to control inertial rate of LOS. [23] Introduced an efficient full-matrix fuzzy logic controller for a gyro mirror line-of-sight stabilization platform. A fuzzy logic based controller and adaptive-neuro fuzzy inference system (ANFIS) have been presented in [19–24] for speed control of DC servo motor. In [25], a comparative study of PID, ANFIS, and hybrid-PID ANFIS controllers has been accomplished for the speed control of brushless direct current motor. In this paper, a self-tuning PID-type fuzzy technique is introduced for a two axes gimbal system which its mathematical model is completely derived using Lagrange equation considering the cross coupling between two channels, the dynamic unbalance, and the base angular velocities. The control aims are mainly to achieve good transient and steady-state

performance with respect to step input commands. The contributions of this paper can be summarized as follows. The complete model of two axes gimbal system is derived assuming that gimbals have mass unbalance as well as considering all inertia disturbances and cross coupling. Then, an applicable adaptive fuzzy controller is designed utilizing simple tuning algorithm which can considerably reduce the overshoot without significant increase in the rise time value. The paper is organized in the following manner. In Section 2, the problem is formulated and the equations of gimbals motion are derived in Section 3. Afterwards, the stabilization loop is investigated and constructed in Section 4. Then, in Section 5 the proposed fuzzy controller is designed. The simulation results are introduced in Section 6. Finally, the conclusion remarks are highlighted in Section 7.

## 2. Problem formulation

The stabilization is usually provided to the sensor by suspending it on the inner gimbal of two axes gimbal system as shown in Fig. 1 [26]. A rate gyro located on the inner gimbal is utilized to measure the angular rates in the two planes of interest. The gyro outputs are used as feedback to torque motors related to the gimbals to provide boresight error tracking and stabilization against base angular motion. The overall control system is constructed utilizing two identical stabilization loops (Fig. 2) for the inner (elevation) and outer (azimuth) gimbals. The control system of two axes gimbal system attempts to align the sensor optical axis in elevation and azimuth planes with a line joining the sensor and target which is called the line of sight (LOS) so that the sensor optical axis is kept nonrotating in an inertial space despite torque disturbances which affect the elevation and azimuth gimbals and basically caused by the base angular motions which are usually imposed by the operating environment. Therefore, the stabilization loop must isolate the sensor from the angular base motion and disturbances that disturb the aim-point, i.e. the output rates of stabilization loops must follow certain input rate commands so that the rate error is made zero. According to Newton's first and second laws, all that is required to prevent an object (sensor) from rotating with respect to inertial space is to ensure that the applied

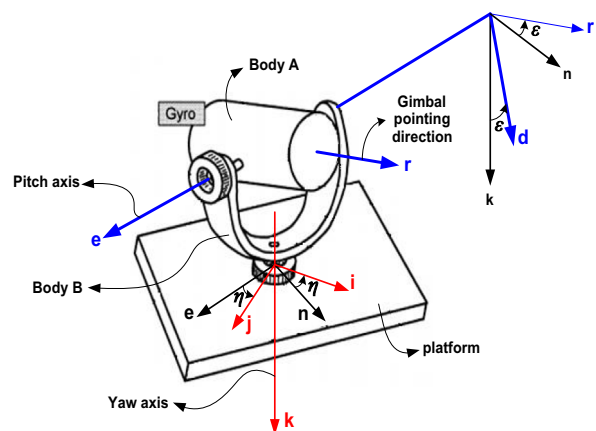


Fig. 1. Two axes gimbal system [23].

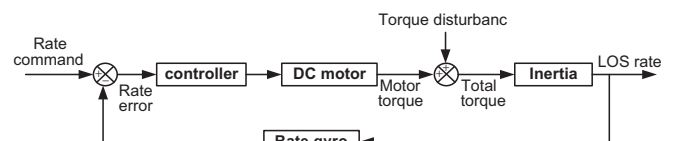


Fig. 2. One axis gimbal stabilization loop.

torque is zero [27]. However, even in well designed and careful electromechanical systems, the operating environment creates numerous sources of torque disturbances that affect on a real mechanism making extreme motion or jitter of line of sight [27]. In such environments, as all control systems, the gimbal control system suffers from problems related to undesirable overshoot, longer settling times and vibrations, and stability. In order to overcome these problems, the gimbal system control loops will be developed using adaptive PID-type fuzzy controller. The elevation and azimuth control loops are related by the cross coupling unit which is built based on the relationships of torques affect the gimbals. The cross coupling express the properties of the gimbal system dynamics and reflects the fact that azimuth gimbal can affect on elevation gimbal even when base body is nonrotating. Also, there is similar impact from elevation gimbal on azimuth gimbal. As a result, the cross coupling is defined as the effect on one axis by the rotation of another [6]. In this paper, the model of two axes gimbal system is obtained and simulated considering the dynamic mass unbalance which is the result of a non-symmetrical mass distribution called Product of Inertia (POI) [6]. The dynamic mass unbalance concept can be indicated by the inertia matrix. If the gimbal has a symmetrical mass distribution with respect to its frame axes, so the gimbal has no dynamic mass unbalance and its inertia matrix is diagonal and vice versa.

### 3. Equations of gimbals motion

In this paper, a two axes gimbal system depicted in Fig. 1 is considered. Three reference frames are identified; frame  $P$  fixed to fuselage body with axes  $(i,j,k)$ , frame  $B$  fixed to azimuth gimbal with axes  $(n,e,k)$ , and frame  $A$  fixed to elevation gimbal with axes  $(r,e,d)$ . The  $r$ -axis coincides with the sensor optical axis. The  $k$  axis is pointing “downwards”. The rotation center is at the frame origin, which is assumed to be the same point for three frames. The transformation matrices in terms of rotation angles  $\varepsilon, \eta$

$${}^B_P C = \begin{bmatrix} \cos \eta & \sin \eta & 0 \\ -\sin \eta & \cos \eta & 0 \\ 0 & 0 & 1 \end{bmatrix}, {}^A_B C = \begin{bmatrix} \cos \varepsilon & 0 & -\sin \varepsilon \\ 0 & 1 & 0 \\ \sin \varepsilon & 0 & \cos \varepsilon \end{bmatrix} \quad (1)$$

where  ${}^B_P C$  is the transformation from frame  $P$  to frame  $B$ . Similarly,  ${}^A_B C$  is the transformation from frame  $B$  to frame  $A$ . The inertial angular velocity vectors of frames  $P, B$ , and  $A$ , respectively are

$${}^P \vec{\omega}_{P/I} = \begin{bmatrix} \omega_{pi} \\ \omega_{pj} \\ \omega_{pk} \end{bmatrix}, {}^B \vec{\omega}_{B/I} = \begin{bmatrix} \omega_{Bn} \\ \omega_{Be} \\ \omega_{Bk} \end{bmatrix}, {}^A \vec{\omega}_{A/I} = \begin{bmatrix} \omega_{Ar} \\ \omega_{Ae} \\ \omega_{Ad} \end{bmatrix} \quad (2)$$

where  $\omega_{pi}, \omega_{pj}, \omega_{pk}$  are the body angular velocities of frame  $P$  in relation to inertial space about  $i, j$ , and  $k$  axes respectively,  $\omega_{Bn}, \omega_{Be}, \omega_{Bk}$  are the azimuth gimbal angular velocities in relation to inertial space about  $n, e$ , and  $k$  axes, respectively, and  $\omega_{Ar}, \omega_{Ae}, \omega_{Ad}$  are the elevation gimbal angular velocities in relation to inertial space about the  $r, e$ , and  $d$  axes, respectively. Inertia matrices of elevation and azimuth gimbals are

$${}^A J_{inner} = \begin{bmatrix} A_r & A_{re} & A_{rd} \\ A_{re} & A_e & A_{de} \\ A_{rd} & A_{de} & A_d \end{bmatrix}, {}^B J_{outer} = \begin{bmatrix} B_n & B_{ne} & B_{nk} \\ B_{ne} & B_e & B_{ke} \\ B_{nk} & B_{ke} & B_k \end{bmatrix} \quad (3)$$

where  $A_r, A_e, A_d$  are elevation gimbal moments of inertia about  $r, e$ , and  $d$  axes,  $A_{re}, A_{rd}, A_{de}$  are elevation gimbal moments products of inertia,  $B_n, B_e, B_k$  are azimuth gimbal moments of inertia about  $n, e$ , and  $k$  axes, and  $B_{ne}, B_{nk}, B_{ke}$  are azimuth gimbal moments products of inertia. Also, it is introduced  $T_{EL}$  as the total external torque about the elevation gimbal  $e$ -axis, and  $T_{AZ}$  as the total external torque about the azimuth gimbal  $k$ -axis. As mentioned above, the

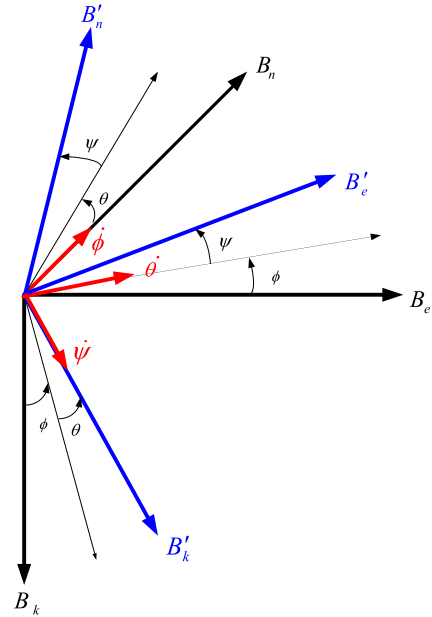


Fig. 3. Azimuth gimbal angular velocities.

aim is to stabilize the gimbal system LOS ( $r$ -axis), i.e. the output rates of stabilization loops  $\omega_{Ae}, \omega_{Ad}$ , which can be measured by a rate gyro placed on the elevation gimbal, must follow the input rate commands  $\omega_{EL}, \omega_{AZ}$ . In general, Euler angles define the position between two related reference frames [28]. For frames  $P$  and  $B$  utilizing the angle  $\eta$ , then between azimuth gimbal frame  $B$  and elevation gimbal frame  $A$  utilizing the angle  $\varepsilon$ , the following relations can be respectively obtained.

**Eq.a :**  $\omega_{Bn} = \omega_{pi} \cos \eta + \omega_{pj} \sin \eta$ ,

**Eq.b :**  $\omega_{Be} = -\omega_{pi} \sin \eta + \omega_{pj} \cos \eta$ ,

**Eq.c :**  $\omega_{Bk} = \omega_{pk} + \dot{\eta}$  (4)

**Eq.a :**  $\omega_{Ar} = \omega_{Bn} \cos \varepsilon - \omega_{Bk} \sin \varepsilon$ ,

**Eq.b :**  $\omega_{Ae} = \omega_{Be} + \dot{\varepsilon}$ ,

**Eq.c :**  $\omega_{Ad} = \omega_{Bn} \sin \varepsilon + \omega_{Bk} \cos \varepsilon$  (5)

The orientation of the gimbal system in an inertial system is completely determined by four independent consecutive rotations  $\phi, \theta, \psi, \varepsilon$  where  $\phi, \theta, \psi$  are Euler rotations of the azimuth gimbal and  $\varepsilon$  is elevation gimbal angle [5]. Then, rotation angles can be taken as generalized coordinates in Lagrange equations. The rotations order is essential [5]. Fig. 3 shows the order of consecutive Euler rotations of azimuth gimbal. By taking the rotations in the order roll ( $\phi$ ), elevation ( $\theta$ ), and azimuth ( $\psi$ ) followed by  $\varepsilon$ , the generalized “forces” corresponding to the coordinates  $\psi$  and  $\varepsilon$  are the external torques  $T_{AZ}$  and  $T_{EL}$  applied to azimuth and elevation gimbals, respectively [5]. The kinetic energy  $T$  of rotating body is given by the scalar product ( $T = \bar{\omega} \times (\bar{H}/2)$ ;  $\bar{H} = J\bar{\omega}$ ); where  $\bar{H}$  the angular momentum,  $\bar{\omega}$  the body inertial rate expressed in the body fixed frame, and  $J$  the body inertia matrix. Thus the total kinetic energy of two axes gimbal system is the sum of kinetic energy of elevation and azimuth gimbals.

$$T = \bar{\omega} \times \frac{\bar{H}}{2} \Big|_A + \bar{\omega} \times \frac{\bar{H}}{2} \Big|_B = \frac{1}{2}(A_r \omega_{Ar}^2 + A_e \omega_{Ae}^2 + A_d \omega_{Ad}^2) + A_{re} \omega_{Ar} \omega_{Ae} + A_{rd} \omega_{Ar} \omega_{Ad} + A_{de} \omega_{Ae} \omega_{Ad} + \frac{1}{2}(B_n \omega_{Bn}^2 + B_e \omega_{Be}^2 + B_k \omega_{Bk}^2) + B_{ne} \omega_{Bn} \omega_{Be} + B_{nk} \omega_{Bn} \omega_{Bk} + B_{ke} \omega_{Be} \omega_{Bk} \quad (6)$$

Based on Fig. 3, the azimuth gimbal angular velocities can be derived as follows

$$\begin{aligned} \omega_{Bn} &= \dot{\phi} \cos \theta \cos \psi + \dot{\theta} \sin \psi, \\ \omega_{Be} &= -\dot{\phi} \cos \theta \sin \psi + \dot{\theta} \cos \psi, \quad \omega_{Bk} = \dot{\phi} \sin \theta + \dot{\psi} \end{aligned} \quad (7)$$

Using (7) and (5) in (6) give the kinetic energy as a function of the generalized coordinates and their time derivatives. Thus, Lagrange equation can be formulated utilizing  $T$  from (6) and equations of motion are obtained. The complete derivation of azimuth relationships is illustrated in Appendix A. Lagrange equation for  $\psi$  is

$$\frac{d}{dt} \left( \frac{\partial T}{\partial \dot{\psi}} \right) - \frac{\partial T}{\partial \psi} = T_{AZ} \quad (8)$$

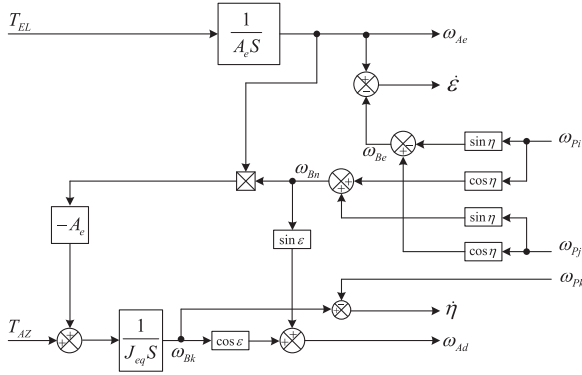


Fig. 4. Simplified two axes gimbal torque relationships introduced in [5].

The equation of azimuth gimbal motion can be derived as a differential equation for  $\omega_{Bk}$  as follows

$$J_{eq} \dot{\omega}_{Bk} = T_{AZ} + T_{d1} + T_{d2} + T_{d3}; \quad T_d = T_{d1} + T_{d2} + T_{d3} \quad (9)$$

After some mathematical operations, Eq. (9) can be converted to a differential equation for  $\omega_{Ad}$  as follows

$$J_{eq} \dot{\omega}_{Ad} = T_{AZ} \cos \varepsilon + T_d \cos \varepsilon + T'_d \quad (10)$$

In [5], Eq. (9) has been simplified assuming that gimbals have no dynamic mass unbalance i.e. ( $A_{re}=A_{rd}=A_{de}=B_{ne}=B_{nk}=B_{ke}=0$ ) as well as applying other choices of inertia parameters ( $A_r=A_d$ ,  $B_n+A_r=B_e$ ). Therefore in [5], the disturbances  $T_d$  have been reduced to one term ( $A_e \omega_{Bn} \omega_{Ae}$ ). Thus, Eq. (9) becomes

$$J_{eq} \dot{\omega}_{Bk} = T_{AZ} - A_e \omega_{Bn} \omega_{Ae} \quad (11)$$

Also, the complete derivation of elevation relationships is illustrated in Appendix B. Lagrange equation for  $\varepsilon$  is

$$\frac{d}{dt} \left( \frac{\partial T}{\partial \dot{\varepsilon}} \right) - \frac{\partial T}{\partial \varepsilon} = T_{EL} \quad (12)$$

The elevation gimbal motion equation is obtained as a differential equation for the elevation rate  $\omega_{Ae}$  as follows

$$\begin{aligned} A_e \dot{\omega}_{Ae} &= T_{EL} + (A_d - A_r) \omega_{Ar} \omega_{Ad} \\ &\quad + A_{rd} (\omega_{Ar}^2 - \omega_{Ad}^2) - A_{de} (\dot{\omega}_{Ad} - \omega_{Ae} \omega_{Ar}) - A_{re} (\dot{\omega}_{Ar} + \omega_{Ae} \omega_{Ad}) \end{aligned} \quad (13)$$

In [5], Eq. (13) has been simplified by eliminating all disturbances assuming that elevation gimbal has no dynamic mass unbalance, i.e. ( $A_{re}=A_{rd}=A_{de}=0$  and  $A_r=A_d$ ). Therefore, Eq. (13) becomes as follows

$$A_e \dot{\omega}_{Ae} = T_{EL} \quad (14)$$

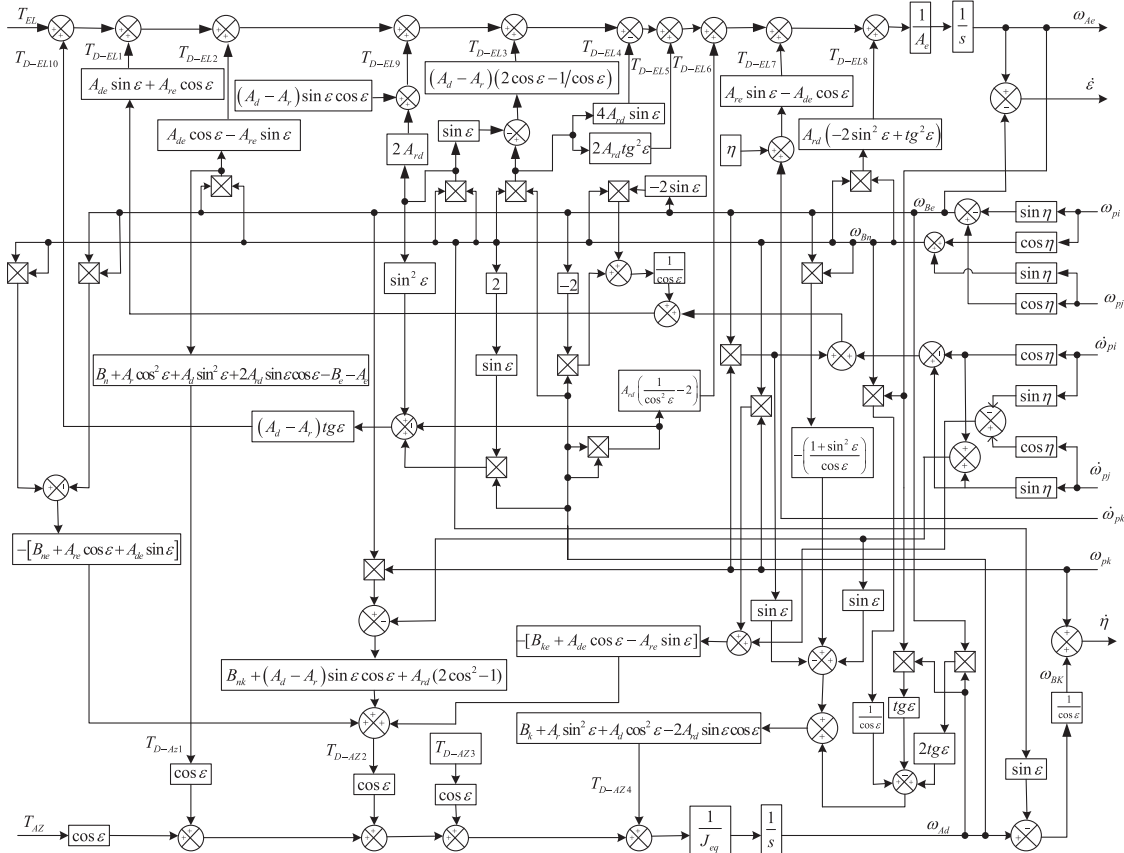


Fig. 5. Complete two axes gimbal torque relationships (cross coupling unit).

Based on (11) and (14), the simplified model obtained in [5] is indicated in Fig. 4. While utilizing Eqs. (10), (A.10), (A.11), (A.12) of azimuth channel in addition to Eqs. (13), (B.4),..., (B.14) of elevation channel, the complete torque relationships of two axes gimbal system introduced in this work is presented in Fig. 5.

Concerning cross coupling, the elevation disturbances (B.3) can be divided into two parts  $T_{D-EL} = T_{B-EL} + T_{C-EL}$  where

$$T_{B-EL} = -(A_{de} \sin \varepsilon + A_{re} \cos \varepsilon)(\dot{\omega}_{Bn} + \omega_{Be}\omega_{Bk}) + (A_{de} \cos \varepsilon - A_{re} \sin \varepsilon)\omega_{Bn}\omega_{Be} + [(A_d - A_r) \cos(2\varepsilon) - 2A_{rd} \sin(2\varepsilon)]\omega_{Bn}\omega_{Bk} + \frac{1}{2}[(A_d - A_r) \sin(2\varepsilon) + 2A_{rd} \cos(2\varepsilon)]\omega_{Bn}^2 \quad (15)$$

$$T_{C-EL} = (A_{re} \sin \varepsilon - A_{de} \cos \varepsilon)\dot{\omega}_{Bk} - \frac{1}{2}(A_d - A_r) \sin(2\varepsilon) + 2A_{rd} \cos(2\varepsilon)\omega_{Bk}^2 \quad (16)$$

It can be seen that the azimuth gimbal may affects the elevation gimbal irrespective of the base body motions because even when the base is nonrotating i.e.,  $\omega_{pi} = \omega_{pj} = \omega_{pk} = 0$  the term  $T_{B-EL}$  is absolutely zero because from (4) we have  $\omega_{Bn} = \omega_{Be} = 0$  but  $\omega_{Bk}$  and consequently the term  $T_{C-EL}$  is not necessarily zero. Therefore, the term  $T_{C-EL}$  is the elevation cross coupling term. Similarly, the disturbances of azimuth channel  $T_d = T_{d1} + T_{d2} + T_{d3}$  can be divided into two parts  $T_d = T_{B-AZ} + T_{C-AZ}$ . Applying the same discussion above, the term  $T_{C-AZ}$  is the azimuth cross coupling term which expresses the effect of elevation gimbal on the azimuth gimbal even when the base is nonrotating.

$$T_{B-AZ} = T_{d1} + T_{d2} + [(A_r - A_d) \cos(2\varepsilon) + 2A_{rd} \sin(2\varepsilon) - A_e]\dot{\omega}_{Bn} + [(A_r - A_d) \sin(2\varepsilon) - 2A_{rd} \cos(2\varepsilon)]\omega_{Be}\omega_{Bk} + (A_{de} \cos \varepsilon - A_{re} \sin \varepsilon)\dot{\omega}_{Be} - (A_{de} \sin \varepsilon + A_{re} \cos \varepsilon)\omega_{Be}^2 \quad (17)$$

$$T_{C-AZ} = (A_{re} \sin \varepsilon - A_{de} \cos \varepsilon)\dot{\omega}_{Ae} + (A_{re} \cos \varepsilon + A_{de} \sin \varepsilon)\omega_{Ae}^2 + [(A_d - A_r) \sin(2\varepsilon) + 2A_{rd} \cos(2\varepsilon)]\omega_{Ae}\omega_{Bk} \quad (18)$$

In [5], Ekstrand has assumed that the inertia cross coupling between channels of gimbal system indicated by (16) and (18) can be eliminated assuming that  $(A_{re} = A_{rd} = A_{de} = 0$  and  $A_r = A_d)$ . While in this paper, this assumption has not been applied and consequently the cross coupling effects have been completely considered.

#### 4. Stabilization loop construction

The components of stabilization loop are indicated in Fig. 2. Although, the researchers tried to utilize and apply many different modern techniques to control inertia stabilization systems, the conventional PID and its constructions are still the most used approach due to their simple structure, cheap costs, simple design and high performance [29]. Therefore, to evaluate the efficiency of proposed fuzzy controller, two PI controllers ( $K_{EL}$  for elevation channel and  $K_{AZ}$  for azimuth one) have been utilized for comparison

$$K_{EL}(s) = 0.09 + \frac{12.5}{s}, K_{AZ}(s) = 0.5 + \frac{12.5}{s} \quad (19)$$

Any servo motion control system should have an actuator module that makes the system to actually perform its function. The most common actuator used to perform this task is the DC servomotor. DC motor is one of the simplest motor types. It is widely preferred for high performance systems requiring minimum torque ripple, rapid dynamic torque, speed responses, high efficiency and good inertia [30]. These motors speedily respond to a command signal by means of a suitable controller. In this kind of motors, the speed control is carried out by changing the supply

**Table 1**  
DC motor specifications [32].

Parameter	Value
Nominal voltage $u_a$	27 V
No load speed $\omega_{nL}$	303 rpm
Terminal resistance $R_a$	4.5 $\Omega$
Terminal inductance $L_a$	0.003 H
Torque constant $K_{TM}$	0.85 Nm/A
Back EMF $K_e$	0.85 V/rad/s
Rotor inertia $J_m$	0.0017 $\text{kg} \times \text{m}^2$
Damping ratio $a_m$	0

**Table 2**  
Gyroscope characteristics [32].

Input rate	From $\pm 40$ to $\pm 1000$ deg/s
Output	AC or DC
Scale factor	Customer specification
Natural frequency	20 to 140 Hz
Damping ratio	0.4 to 1.0

voltage of the motor [31]. DC motor from NORTHROP GRUMMAN Company (Table 1) is utilized. The transfer function of DC motor can be obtained as follows

$$G_m(s) = \frac{\omega_m(s)}{u_a(s)} = \frac{K_{TM}}{(L_a s + R_a) \times (J_m^* s + a_m^*) + K_e K_{TM}} = \frac{24637.68}{s^2 + 1500s + 20942}; a_m^* = 0 \quad (20)$$

where  $\omega_m$  is motor's angular velocity, and  $u_a$  is motor's armature voltage. Also,  $J_m^* = J_m + J_L$  and  $a_m^* = a_m + a_L$  where  $J_L$  is platform's moment of inertia, and  $a_L$  is the load's damping ratio. The platform represents the motor load, which is attached to the output of the gears or directly to the shaft motor. The platform is modelled based on its moment of inertia  $J_L$  that depends on its dimensions and its position respect to the axis of rotation. In this paper, a discus is proposed to represent the platform where its mass  $M = 1$  kg and radius  $r = 14$  cm, so  $J_L = 9.8 \times 10^{-3} \text{ kg} \times \text{m}^2$ . In this paper, the 475 T rate gyroscope from the US Dynamics company (Table 2) is considered. The rate gyro can be modelled in the second order system typically [33]. For the gyro of natural frequency  $\omega_n = 50$  Hz, and damping ratio  $\zeta = 0.7$  the gyro transfer function is

$$G_{Gyro}(s) = \frac{\omega_n^2}{(s^2 + 2\zeta\omega_n s + \omega_n^2)} = \frac{2500}{(s^2 + 70s + 2500)} \quad (21)$$

#### 5. Proposed controller design

The drawback of the conventional PID appears when the control system works under variable conditions. Therefore, in systems such as proposed inertia stabilization system, PID controller cannot maintain the good performance unless the controller parameters are retuned. The progress report [34] pointed out that the adaptive control technique is the future development direction of LOS inertia stabilization systems. In such environments, the overshoot in gimbal system response is inevitable challenge that must be solved because it degrades the control system performance. The solution difficulty results from the fact that the overshoot and rise time usually conflict each other and they cannot be reduced simultaneously. The conventional PID controller and its different structures have been widely used for the speed control of DC motor drives and gimbal systems

(especially PI controller). Although PI controller keeps a zero steady-state error to a step change in reference, but it also has undesirable speed overshoot (high starting overshoot), slow response due to sudden change in load torque, and sensitivity to controller gains [19]. Thus, utilizing conventional control approaches like classical PID (PI) can solve this problem approximately and slightly decrease the overshoot but absolutely at the expense of increasing the rise time value. Therefore, the need to improve PID (PI) performance has insistently appeared. In this paper, the gimbal system control loops will be developed using adaptive PID-type fuzzy controller. Fuzzy logic controller belongs to intelligent control system which combines the technique from the field of artificial intelligent with those of control engineering to design autonomous system that can sense, reason and plan, learn and act in intelligent manner [35]. Basically, fuzzy controller comprises of four main components, fuzzification interface, knowledge base, inference mechanism and defuzzification interface [35]. Fig. 6 shows components of fuzzy logic controller. Fuzzification converts input data into suitable linguistic values, while defuzzification yields a non fuzzy control action from inferred fuzzy control action. The rule base is a decision making logic, which is simulating a human decision process, inters fuzzy control action from the knowledge of the control rules and linguistic variable definitions. The fuzzified input variables are used by the inference mechanism to evaluate control rules stored in the fuzzy rule-base. The result of this evaluation is a single fuzzy set or several fuzzy sets. In literature, various structures of fuzzy PID (including PI and PD) controllers and fuzzy non-PID controllers have been proposed. The conventional fuzzy PID controller needs three inputs and the rule base has three dimensions, it is more difficult to design the rule-base. On the other hand, the fuzzy PD type controller difficultly eliminates the steady state error which can be completely removed using fuzzy PI type controller. The fuzzy PI type controller, however, achieves poor performance in transient response especially when it is used for higher order process [36]. In order to obtain the advantages of these two controllers, it is useful to combine them in what can be named fuzzy PID type controller that has just two inputs and two dimensions rule base. Fig. 7 shows the construction of the proposed fuzzy PID type controller which will be utilized in this paper instead of the conventional PID. Where  $K_e, K_d$  are the input scaling factors of error and change of error, and  $\beta, \alpha$  are the output scaling factors. Based on what has been made in [37], the relation

between input and output variables of fuzzy parameters is

$$U = A + PE + D\dot{E}; \quad E = K_e e, \dot{E} = K_d \dot{e} \tag{22}$$

The output of fuzzy PID type controller is

$$u_c = \alpha U + \beta \int U dt = \alpha A + \beta A t + \alpha K_e P e + \beta K_d D e + \beta K_e P \int e dt + \alpha K_d D \dot{e} \tag{23}$$

These control components can be divided into proportional  $\alpha K_e P + \beta K_d D$ , integral  $\beta K_e P$ , and derivative  $\alpha K_d D$ . The design parameters of the fuzzy PID controllers can be summarized within two groups [38]: Structural parameters, and tuning parameters. Structural parameters, which are usually determined during off-line design, include input/output variables to fuzzy inference, fuzzy linguistic sets, membership functions, fuzzy rules, inference mechanism and defuzzification mechanism. Tuning parameters include scaling factors and parameters of membership functions. The selection of tuning parameters is a critical task, which is usually carried out through trail and error or using some training data. Also, these parameters can be calculated during on-line adjustments of the controller to enhance the process performance, as well as to accommodate the adaptive capability to system uncertainty and process disturbance [36]. The fuzzy controller is regarded adaptive if any one of its tuneable parameters (scaling factors, membership functions, and rules) changes when the controller is being used; otherwise it is conventional fuzzy controller. An adaptive fuzzy controller that fine tunes an already working controller by modifying either its scaling factors or membership functions or, both of them is called a self-tuning fuzzy controller. On the other hand, when a fuzzy controller is tuned by automatically changing its rules then it is called a self-organizing fuzzy controller [39]. Of the various tuning parameters, scaling factors have the highest priority due to their global effect on the control performance [39]. Therefore, the proposed controller is designed as self-tuning fuzzy controller which is tuned by modifying its input scaling factors. Seven triangular membership functions indicated in Fig. 8 are used for the fuzzification of the inputs ( $e, \dot{e}$ ) and output ( $U$ ) variables. For the membership functions used, NL, NM, NS, ZR, PS, PM, PL denotes negative large, negative medium, negative small, zero, positive small, positive medium, and positive large, respectively. All membership

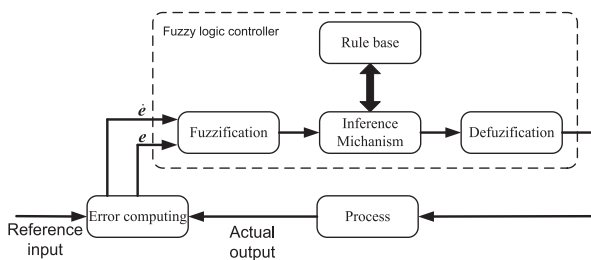


Fig. 6. Components of fuzzy logic controller.

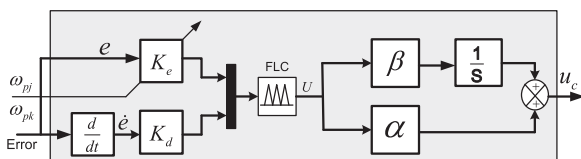


Fig. 7. Simulink model of fuzzy PID type controller.

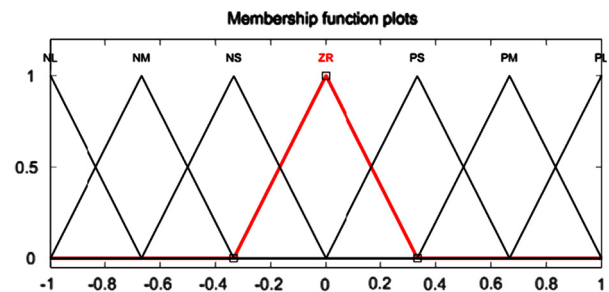


Fig. 8. Membership functions of  $e, \dot{e}$  and  $U$ .

Table 3  
Fuzzy PID type rule base.

$e/\dot{e}$	NL	NM	NS	ZR	PS	PM	PL
NL	LN	LN	LN	LN	MN	SN	ZE
NM	LN	LN	LN	MN	SN	ZE	SP
NS	LN	LN	MN	SN	ZE	SP	MP
ZR	LN	MN	SN	ZE	SP	MP	LP
PS	MN	SN	ZE	SP	MP	LP	LP
PM	SN	ZE	SP	MP	LP	LP	LP
PL	ZE	SP	MP	LP	LP	LP	LP

functions are defined on the  $[-1,1]$  closed interval. All the scaling factors  $(K_e, K_d, \beta, \alpha)$  are used to map the related crisp values to their fuzzy universe of discourse. The control output  $U$  can be determined from the center of gravity method. The rules of the proposed controller are expressed as follows: If  $\{e$  is ZR and  $\dot{e}$  is ZR $\}$ , then  $\{U$  is ZR $\}$ . The rule base is constructed based on the following approach: when the system output is far from the desired output i.e.  $e$  is PL and  $\dot{e}$  is ZR then  $U$  is selected to be PL in order to decrease the error value and bring the system state to the desired value rapidly. If the error  $e$  is ZR and it tends to increase due to the nonzero  $\dot{e}$  thus,  $U$  should not be zero (for example, if  $e$  is ZR and  $\dot{e}$  is NM then  $U$  is NM). When both  $e$  and  $\dot{e}$  are zero which is the desired case and the system does not need any control input therefore,  $U$  is selected to be ZR. The fuzzy PID type control rules are shown in Table 3. In general, the inertial stabilization systems work under variable conditions especially the base angular velocities. The most dominant parameters in elevation and azimuth channels are  $\omega_{pj}, \omega_{pk}$ , respectively. It is realized that whenever  $\omega_{pj}, \omega_{pk}$  increase, the system response overshoot unacceptably increases. It is known that the integral and proportional parameters have a great influence on the stable and dynamic performance of control system which is usually evaluated using the concepts of maximum overshoot, rise time, settling time, and steady state error. It is noted that the input scaling factor  $K_e$  exists in both integral and proportional terms, and it is therefore selected to be tuned on-line based on the values of  $\omega_{pj}, \omega_{pk}$ , while the other tuning parameters  $\alpha, \beta, K_d$  are adjusted

off-line based on the knowledge about the process to be controlled and sometimes through trial and error to achieve the best possible control performance. Table 4 indicates the values of these off-line adjusted parameters. This on-line tuning operation improves further the performance of the transient and steady states of the two axes gimbal system using the proposed fuzzy PID type controller. In order to establish the on-line tuning of  $K_e$ , a parametric study is applied to obtain the most suitable value of  $K_e$  against every value of the angular velocities  $\omega_{pj}, \omega_{pk}$  along the interval  $[0-15]$  deg/s. As a result of this parametric study, two relationships  $K_e(\omega_{pj})$  and  $K_e(\omega_{pk})$  can be obtained for elevation and azimuth channels, respectively

$$K_e(\omega_{pj}) = -0.0093\omega_{pj}^2 + 0.0371\omega_{pj} + 0.7933,$$

$$K_e(\omega_{pk}) = -0.0013\omega_{pk}^2 - 0.0057\omega_{pk} + 0.6293 \quad (24)$$

From (24), it is noted that unlike to most of adaptive controllers which are often built using complex tuning algorithms, the proposed fuzzy controller simply achieves self tuning operation based on the base rate values which can be measured by inertial measurement unit (IMU). Therefore, the proposed self-tuning fuzzy PID type controller is completely applicable. Although many control approaches have been widely used to improve the control system performance, the proposed fuzzy PID controller aims to considerably reduce the overshoot of two axes gimbal system response without significant increase in the rise time unlike to most of controllers which usually reduce the overshoot at the expense of the rise time value.

**Table 4**  
Off-line adjusted parameters.

Parameter	$K_d$	$\alpha$	$\beta$
Elevation	0.01	0.08	13
Azimuth	0.02	0.25	25

**6. Simulation results**

Based on what has been carried out above, the control system of the two axes gimbal assembly can be accomplished using two stabilization loops with a cross coupling unit between them. The overall simulation model of the gimbal system has been prepared

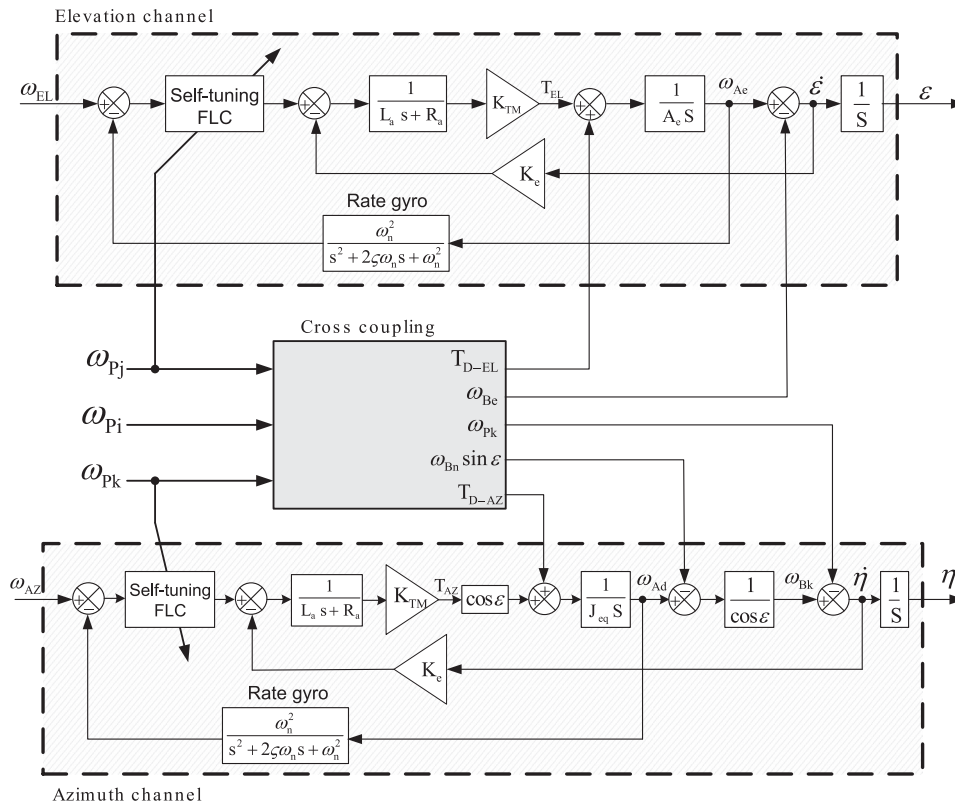


**Fig. 9.** Two axes stabilization loops.

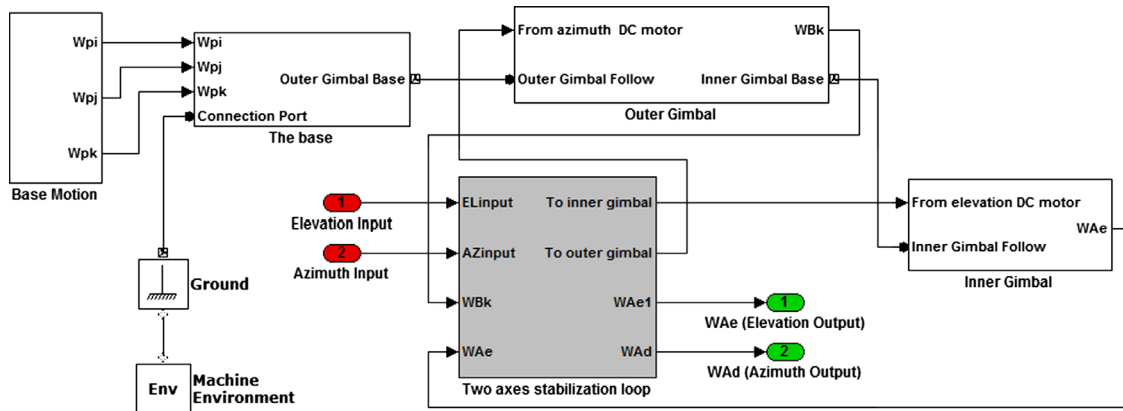


Fig. 10. Block diagram of SimMechanics model.

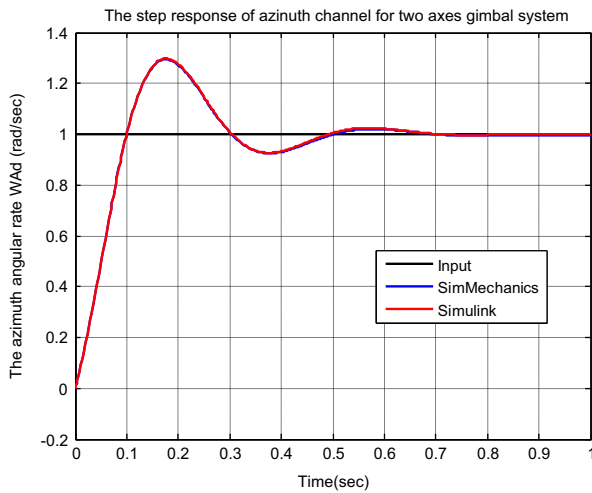


Fig. 11. The step response of azimuth, channel.

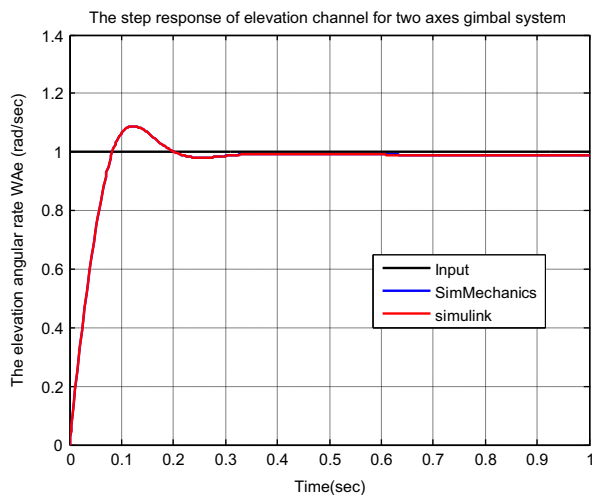


Fig. 12. The step response of elevation, channel.

in MATLAB/Simulink environment utilizing the proposed self-tuning fuzzy PID type controller as depicted in Fig. 9.

### 6.1. Validation test and disturbance analysis

The two axes gimbal system is validated using SimMechanics model shown in Fig. 10. Responses obtained using both Simulink

and SimMechanics for azimuth and elevation channels are displayed in Figs. 11 and 12, respectively. It is clear that the two responses of elevation and azimuth channels are completely identical. Therefore, this conformity ensures the validity and correction of the gimbal system introduced in this research. The torque disturbance affect in the elevation and azimuth channels have been obtained in details and indicated by Eqs. (B.4) and (A.9), respectively. It is clear that the base angular motions ( $\omega_{pi}, \omega_{pj}, \omega_{pk}$ ) represent the most important source of torque disturbances  $T_{D-EL}$ ,  $T_{D-AZ}$  which have been added with elevation and azimuth loops respectively as shown in the overall simulink model indicated in Fig. 9. The interested torques in elevation and azimuth channels can be obtained as shown in Fig. 13 which shows that the closed control loop in elevation channel (and azimuth channel) generates a control torque (motor torque)  $T_{EL}$  (and  $T_{AZ}$ ) which tries to eliminate the effect of disturbance torque  $T_{D-EL}$  (and  $T_{D-AZ}$ ) so that the total torque applied on the elevation gimbal (and azimuth gimbal) is close to zero as much as possible in order to prevent the object (sensor) from rotating with respect to the inertial space or in other words to provide stability to the sensor and this is exactly what has been previously accomplished according to Newton's laws.

### 6.2. Performance comparison of fuzzy PID type and conventional PI controllers

Having designed a fuzzy PID type controller, it is important to validate its performance and compare it with conventional PI controller. Actually, the transient response is considered one of the most important characteristics of control systems. Therefore, in this paper, the transient response of gimbal system has been used to analyze the performance of the conventional PI and proposed fuzzy controllers. This analysis has been made based on three transient response specifications; the rise time  $t_r$  (10 to 90%) that indicates the swiftness of response, the settling time  $t_s$  (within 2%) and the maximum percent overshoot (ov) that describe the closeness of response. Also, the overshoot directly indicates the relative stability of the system. The transient response analysis has been carried out using a rate input commands in elevation and azimuth channels equal to  $\omega_{EL} = \omega_{AZ} = 10$  deg/s, while the base angular velocities can be changed along the interval  $\omega_{pj} = \omega_{pk} = [0 - 14]$  deg/s. Based on the analysis results indicated in Table 5, it can be noted that rise times of both conventional PI and fuzzy PID type controllers are kept almost at the same value but with a considerably reduced overshoot and much improved overall performance in case of fuzzy PID type controller. Further more, in some cases the proposed fuzzy controller could mainly decrease the response overshoot with

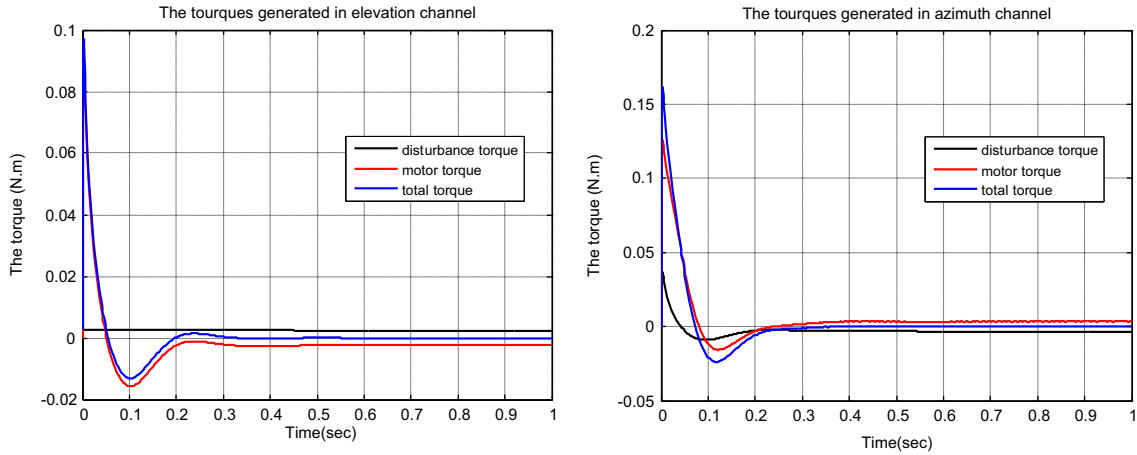


Fig. 13. Torques generated in elevation loop (left), and azimuth loop (right).

Table 5  
Transient response analysis results of elevation and azimuth channels.

$\omega_{pj}$ (deg/s)	Elevation channel						Azimuth channel					
	Conventional PI controller			Fuzzy PID type controller			Conventional PI controller			Fuzzy PID type controller		
	ov (%)	$t_s$ (s)	$t_r$ (s)	ov (%)	$t_s$ (s)	$t_r$ (s)	ov (%)	$t_s$ (s)	$t_r$ (s)	ov (%)	$t_s$ (s)	$t_r$ (s)
2	9.7	0.19	0.059	0	0.13	0.086	6.7	0.16	0.052	0	0.13	0.081
4	15.1	0.17	0.042	0	0.1	0.064	15.2	0.17	0.041	0	0.11	0.072
6	24.3	0.16	0.031	0	0.07	0.046	25.1	0.18	0.035	0	0.08	0.059
8	36.2	0.16	0.023	2	0.05	0.034	35.8	0.19	0.029	2.8	0.06	0.049
10	50	0.15	0.016	2.3	0.03	0.025	47.1	0.2	0.024	6.6	0.11	0.041
12	64.6	0.16	0.014	16	0.127	0.014	58.8	0.21	0.021	10.8	0.12	0.034
14	80	0.15	0.012	18.6	0.125	0.012	70.7	0.22	0.019	6.2	0.16	0.031

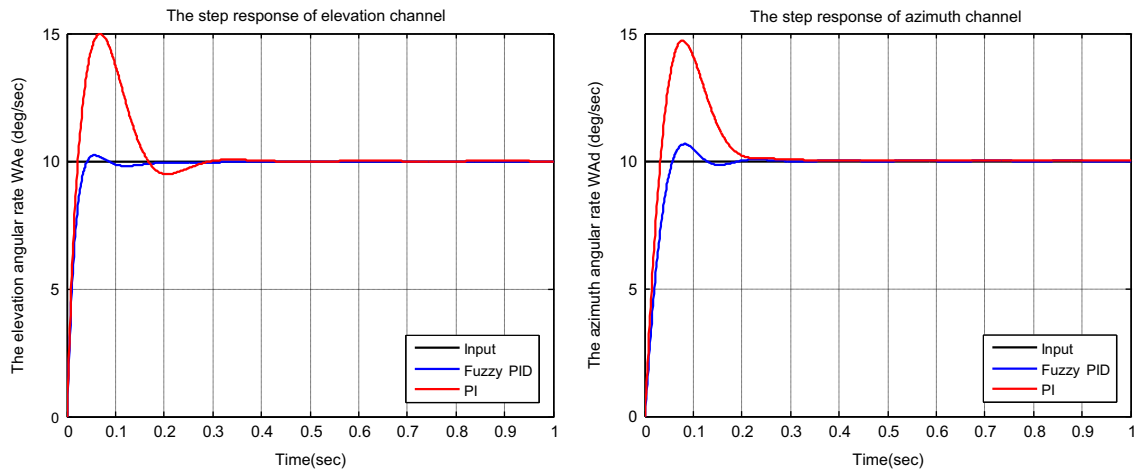


Fig. 14. Step response for  $\omega_{pj} = \omega_{pk} = 10$  deg/s in elevation channel (left), and azimuth channel (right).

maintaining the same rise time value as compared with PI controller. For example, Table 5 indicates that for  $\omega_{pj} = 12$  deg/s the overshoot of elevation response has been reduced from 64.6% (utilizing PI controller) to 16% (utilizing fuzzy PID controller) while the rise time for both controllers was the same  $t_r = 0.012$  s. The same case can be noted in Table 5 for  $\omega_{pj} = 14$  deg/s. As an example, one system response is displayed in Fig. 14 to reflect clearly and visually the efficiency of the fuzzy PID type controller as compared to the conventional PI. On the other hand, in order to support the performance analysis made by means of transient response specifications as mentioned above, a quantitative study

of error analysis has been achieved utilizing three frequently used error integral criteria; integral square error (ISE), integral absolute error (IAE), and integral of time-multiplied absolute error (ITAE) which they are

$$ISE = \int_0^t |e(t)|^2 dt, \quad AIE = \int_0^t |e(t)| dt, \quad ITAE = \int_0^t t|e(t)| dt \quad (25)$$

where  $e(t)$  is the measured error. The errors at the beginning of response can be sufficiently indicated by IAE and with less efficiency for the steady state duration. While ITAE keeps account of errors at the beginning and emphasizes the steady state.

**Table 6**  
Error analysis results of elevation and azimuth channels.

$\omega_{pj}$ (deg/s)	Elevation channel						Azimuth channel					
	Conventional PI controller			Fuzzy PID type controller			Conventional PI controller			Fuzzy PID type controller		
	IAE	ISE	ITEA	IAE	ISE	ITEA	IAE	ISE	ITEA	IAE	ISE	ITEA
2	0.01237	0.00147	0.00068	0.01253	0.001588	0.00057	0.00113	0.0014	0.00052	0.01318	0.0017	0.00061
4	0.01157	0.00127	0.00068	0.01046	0.00133	0.0004	0.0115	0.0013	0.00062	0.0119	0.0015	0.00051
6	0.0118	0.00119	0.00078	0.0092	0.001165	0.00033	0.0122	0.00129	0.00076	0.0109	0.00141	0.00044
8	0.0128	0.00123	0.00095	0.00846	0.001	0.0003	0.01334	0.00135	0.00094	0.0102	0.00131	0.0004
10	0.01425	0.00137	0.00116	0.00816	0.0001	0.00035	0.01472	0.00148	0.00115	0.0098	0.00122	0.00038
12	0.01606	0.00162	0.0014	0.00736	0.00086	0.00028	0.0163	0.00168	0.00136	0.00972	0.00116	0.00042
14	0.0181	0.00198	0.0016	0.00747	0.00084	0.00043	0.018	0.00195	0.0016	0.00912	0.0011	0.0004

Therefore, integral criteria IAE and ITAE are considered because they respectively reflect the transient and steady state characteristics of the control system, The values of error integral criteria obtained for elevation and azimuth channels are provided in Table 6 which indicates that the error in fuzzy PID controller is minimum as compared to PI controller which shows the superiority of the proposed fuzzy controller.

## 7. Conclusion

A two axes gimbal system was proposed and its mathematical model derived utilizing Lagrange equation considering the base angular rates, the dynamic mass unbalance, and the cross coupling between elevation and azimuth channels. Then, the stabilization loop was introduced and a self-tuning fuzzy PID type controller was designed. The overall control system has been created and simulated using MATLAB/Simulink and SimMechanics tools to confirm the validity and correction of the proposed system. The torque disturbance has been analysed, then the performance of fuzzy PID type controller has been tested using transient response analysis and a quantitative study of error analysis. Based on the results obtained, the following observations can be remarked. First, the proposed self tuning operation provides good adaptivity to the gimbal system which offers high performance despite of the torque disturbances so that it can be utilized more efficiently in dynamical environment that usually imposes large variable base rates. Then, the proposed fuzzy controller can reduce the response settling time as compared with the conventional PI controller. Finally, the proposed fuzzy controller improves the closeness of system response and support the system relative stability by reducing the response overshoot considerably without increasing the response rise time dramatically i.e. without largely abaissement or weakening the swiftness of system response like to what usually take place when the conventional PID is used.

## Appendix A. Azimuth channel torque relationships

Utilizing Eqs. (5) and (7) gives

$$\begin{aligned} \frac{\partial \omega_{Bn}}{\partial \dot{\psi}} &= 0, \frac{\partial \omega_{Be}}{\partial \dot{\psi}} = 0, \frac{\partial \omega_{Bk}}{\partial \dot{\psi}} = 1, \frac{\partial \omega_{Bn}}{\partial \psi} = \omega_{Be}, \frac{\partial \omega_{Be}}{\partial \psi} = -\omega_{Bn}, \frac{\partial \omega_{Bk}}{\partial \psi} = 0 \\ \frac{\partial \omega_{Ar}}{\partial \dot{\psi}} &= -\sin \varepsilon, \frac{\partial \omega_{Ae}}{\partial \dot{\psi}} = 0, \frac{\partial \omega_{Ad}}{\partial \dot{\psi}} = \cos \varepsilon, \frac{\partial \omega_{Ar}}{\partial \psi} = \omega_{Be} \cos \varepsilon, \frac{\partial \omega_{Ae}}{\partial \psi} \\ &= -\omega_{Bn}, \frac{\partial \omega_{Ad}}{\partial \psi} = \omega_{Be} \sin \varepsilon \end{aligned} \quad (A.1)$$

Using (A.1), the two terms in Eq. (8) left side are converted into

$$\frac{\partial T}{\partial \dot{\psi}} = -(A_r \omega_{Ar} + A_{re} \omega_{Ae} + A_{rd} \omega_{Ad}) \sin \varepsilon$$

$$+(A_{rd} \omega_{Ar} + A_{de} \omega_{Ae} + A_d \omega_{Ad}) \cos \varepsilon + B_{nk} \omega_{Bn} + B_{ke} \omega_{Be} + B_k \omega_{Bk} \quad (A.2)$$

$$\begin{aligned} \frac{\partial T}{\partial \dot{\psi}} &= -\omega_{Bn}(B_{ne} \omega_{Bn} + B_e \omega_{Be} + B_{ke} \omega_{Bk} + A_{re} \omega_{Ar} + A_e \omega_{Ae} + A_{de} \omega_{Ad}) \\ &+ \omega_{Be}(B_n \omega_{Bn} + B_{ne} \omega_{Be} + B_{nk} \omega_{Bk}) \\ &+ \omega_{Be}(A_r \omega_{Ar} + A_{re} \omega_{Ae} + A_{rd} \omega_{Ad}) \cos \varepsilon \\ &+ \omega_{Be}(A_{rd} \omega_{Ar} + A_{de} \omega_{Ae} + A_d \omega_{Ad}) \sin \varepsilon \end{aligned} \quad (A.3)$$

Based on Eqs. (A.2), (A.3), and (5) the equation of azimuth gimbal motion can be derived as follows

$$J_{eq} \dot{\omega}_{Bk} = T_{Az} + T_{d1} + T_{d2} + T_{d3} \quad (A.4)$$

where  $T_d = T_{d1} + T_{d2} + T_{d3}$  represents different azimuth gimbal inertia disturbances,  $J_{eq}$  is the instantaneous moment of inertia about the  $k$ -axis. All components are defined as follows

$$J_{eq} = B_k + A_r \sin^2 \varepsilon + A_d \cos^2 \varepsilon - A_{rd} \sin(2\varepsilon) \quad (A.5)$$

$$T_{d1} = [B_n + A_r \cos^2 \varepsilon + A_d \sin^2 \varepsilon + A_{rd} \sin(2\varepsilon) - (B_e + A_e)] \omega_{Bn} \omega_{Be} \quad (A.6)$$

$$\begin{aligned} T_{d2} &= -[B_{nk} + (A_d - A_r) \sin \varepsilon \cos \varepsilon + A_{rd} \cos(2\varepsilon)] (\dot{\omega}_{Bn} - \omega_{Be} \omega_{Bk}) \\ &- (B_{ke} + A_{de} \cos \varepsilon - A_{re} \sin \varepsilon) (\dot{\omega}_{Be} + \omega_{Bn} \omega_{Bk}) \\ &- (B_{ne} + A_{re} \cos \varepsilon + A_{de} \sin \varepsilon) (\omega_{Bn}^2 - \omega_{Be}^2) \end{aligned} \quad (A.7)$$

$$\begin{aligned} T_{d3} &= \ddot{\varepsilon}(A_{re} \sin \varepsilon - A_{de} \cos \varepsilon) + \dot{\varepsilon}[(A_r - A_d)(\omega_{Bn} \cos(2\varepsilon) - \omega_{Bk} \sin(2\varepsilon))] \\ &+ \dot{\varepsilon}[2A_{re}(\omega_{Bn} \sin(2\varepsilon) + \omega_{Bk} \cos(2\varepsilon))] \\ &+ \dot{\varepsilon}[(A_{de} \sin \varepsilon + A_{re} \cos \varepsilon)(\omega_{Ae} + \omega_{Be}) - A_e \omega_{Bn}] \end{aligned} \quad (A.8)$$

Inserting  $\dot{\omega}_{Bk}$  obtained from (5c) in (A.4) converts it into a differential equation for the elevation rate  $\omega_{Ad}$  as

$$\begin{aligned} J_{eq} \dot{\omega}_{Ad} &= T_{Az} \cos \varepsilon + T_d \cos \varepsilon + T'_d; \\ T'_d &= J_{eq} [\dot{\omega}_{Bn} \sin \varepsilon + \omega_{Ar}(\omega_{Ae} - \omega_{Be})]; \\ T_{D-AZ} &= (T_{d1} + T_{d2} + T_{d3}) \cos \varepsilon + T'_d \end{aligned} \quad (A.9)$$

where  $T_{D-AZ}$  represents the disturbances affected on azimuth gimbal. The term  $T_{d1}$  will be denoted as  $T_{D-AZ1}$ . Then, using  $\dot{\omega}_{Bn}$  from (4a),  $\omega_{Bk}$  from (5c),  $\dot{\omega}_{Be}$  from (4b), and (5b) the terms  $T_{d2}$  and  $T_{d3}$  are respectively denoted by

$$\begin{aligned} T_{D-AZ2} &= [B_{nk} + (A_d - A_r) \sin \varepsilon \cos \varepsilon + A_{rd}(2 \cos^2 \varepsilon - 1)] \\ &\times (-\dot{\omega}_{pj} \sin \eta - \dot{\omega}_{pi} \cos \eta + \omega_{Be} \omega_{pk}) \\ &- (B_{ne} + A_{re} \cos \varepsilon + A_{de} \sin \varepsilon) (\omega_{Bn}^2 - \omega_{Be}^2) \\ &- (B_{ke} + A_{de} \cos \varepsilon - A_{re} \sin \varepsilon) (\dot{\omega}_{pj} \cos \eta - \dot{\omega}_{pi} \sin \eta + \omega_{Bn} \omega_{pk}) \end{aligned} \quad (A.10)$$

$$\begin{aligned} T_{D-AZ3} &= \dot{\omega}_{Ae}(A_{re} \sin \varepsilon - A_{de} \cos \varepsilon) \\ &+ (A_{de} \cos \varepsilon - A_{re} \sin \varepsilon) (\dot{\omega}_{pj} \cos \eta - \dot{\omega}_{pi} \sin \eta) \\ &+ \omega_{Ad} \omega_{Bn} (A_{de} - A_{re} \tan \varepsilon) + \omega_{Bn}^2 (A_{re} \tan \varepsilon - A_{de}) \sin \varepsilon \end{aligned}$$

$$\begin{aligned}
 &+ 2A_{re}(\omega_{Ae} - \omega_{Be})\omega_{Bn}tg\epsilon + 2\omega_{Ad}\omega_{Be}(A_r - A_d) \sin \epsilon \\
 &+ 2A_{re}\omega_{Ad}(\omega_{Ae} - \omega_{Be})\left(2 \cos \epsilon - \frac{1}{\cos \epsilon}\right) \\
 &+ (\omega_{Ae} - \omega_{Be})(A_{de} \sin \epsilon + A_{re} \cos \epsilon)(\omega_{Ae} + \omega_{Be}) \\
 &- A_e\omega_{Bn} + \omega_{Ae}\omega_{Bn}(A_r - A_d) \tag{A.11}
 \end{aligned}$$

From (5a) we have  $\omega_{Ar} = -\omega_{Ad}tg\epsilon + (\omega_{Bn}/\cos \epsilon)$ , then using  $\omega_{Bk}$  from (5c), and  $\dot{\omega}_{Bn}$  from (4a), the term  $T_d$  denoted by

$$\begin{aligned}
 T_{D-AZ4} = J_{eq} \left[ -\omega_{Be}\omega_{Bn} \left( \frac{1 + \sin^2 \epsilon}{\cos \epsilon} \right) - \omega_{Ad}\omega_{Ae}tg\epsilon \right. \\
 \left. + (\dot{\omega}_{p_i} \cos \eta + \dot{\omega}_{p_j} \sin \eta) \sin \epsilon - \omega_{Be}\omega_{p_k} \sin \epsilon \right. \\
 \left. + \frac{\omega_{Ae}\omega_{Bn}}{\cos \epsilon} + 2\omega_{Ad}\omega_{Be}tg\epsilon \right] \tag{A.12}
 \end{aligned}$$

**Appendix B. Elevation channel torque relationships**

From Eq. (5) we have

$$\frac{\partial \omega_{Ar}}{\partial \dot{\epsilon}} = 0, \frac{\partial \omega_{Ae}}{\partial \dot{\epsilon}} = 1, \frac{\partial \omega_{Ad}}{\partial \dot{\epsilon}} = 0, \frac{\partial \omega_{Ar}}{\partial \dot{\epsilon}} = -\omega_{Ad}, \frac{\partial \omega_{Ae}}{\partial \dot{\epsilon}} = 0, \frac{\partial \omega_{Ad}}{\partial \dot{\epsilon}} = \omega_{Ar} \tag{B.1}$$

Using (B.1) in the kinetic energy for elevation gimbal  $T = (\bar{\omega} \times (\bar{H}/2))_A$ , the two terms in Eq. (12) left side are

$$\begin{aligned}
 \frac{\partial T}{\partial \dot{\epsilon}} &= A_e\omega_{Ae} + A_{re}\omega_{Ar} + A_{de}\omega_{Ad}, \\
 \frac{\partial T}{\partial \epsilon} &= \omega_{Ar}\omega_{Ad}(A_d - A_r) - A_{re}\omega_{Ad}\omega_{Ae} - A_{rd}(\omega_{Ar}^2 - \omega_{Ad}^2) + A_{de}\omega_{Ar}\omega_{Ae} \tag{B.2}
 \end{aligned}$$

Using (B.2) in (12) gives the elevation gimbal motion equation as a differential equation for  $\omega_{Ae}$  as follows

$$\begin{aligned}
 A_e\dot{\omega}_{Ae} = T_{EL} + (A_d - A_r)\omega_{Ar}\omega_{Ad} + A_{rd}(\omega_{Ar}^2 - \omega_{Ad}^2) - A_{de}(\dot{\omega}_{Ad} - \omega_{Ae}\omega_{Ar}) \\
 - A_{re}(\dot{\omega}_{Ar} + \omega_{Ae}\omega_{Ad}); T_{D-EL} = (A_d - A_r)\omega_{Ar}\omega_{Ad} \\
 + A_{rd}(\omega_{Ar}^2 - \omega_{Ad}^2) - A_{de}(\dot{\omega}_{Ad} - \omega_{Ae}\omega_{Ar}) - A_{re}(\dot{\omega}_{Ar} + \omega_{Ae}\omega_{Ad}) \tag{B.3}
 \end{aligned}$$

The elements of inertia matrix form the disturbance term  $T_{D-EL}$ . Using  $\dot{\omega}_{Bn}$  from (4a),  $\dot{\omega}_{Bk}$  from (5c), and (5) converts the disturbance term  $T_{D-EL}$  into the following form

$$\begin{aligned}
 T_{D-EL} = T_{D-EL1} + T_{D-EL2} + T_{D-EL3} + T_{D-EL4} + T_{D-EL5} \\
 + T_{D-EL6} + T_{D-EL7} + T_{D-EL8} + T_{D-EL9} + T_{D-EL10} \tag{B.4}
 \end{aligned}$$

$$\begin{aligned}
 T_{D-EL1} = (A_{de} \sin \epsilon + A_{re} \cos \epsilon) \left[ \frac{-2\omega_{Be}\omega_{Ad} - 2\omega_{Be}\omega_{Bn} \sin \epsilon}{\cos \epsilon} \right. \\
 \left. + \omega_{Be}\omega_{p_k} - \dot{\omega}_{p_i} \cos \eta + \dot{\omega}_{p_j} \sin \eta \right] \tag{B.5}
 \end{aligned}$$

$$T_{D-EL2} = \omega_{Be}\omega_{Bn}(A_{de} \cos \epsilon - A_{re} \sin \epsilon) \tag{B.6}$$

$$T_{D-EL3} = (A_d - A_r) \left[ 2 \cos \epsilon - \frac{1}{\cos \epsilon} \right] [\omega_{Bn}\omega_{Ad} - \omega_{Bn}^2 \sin \epsilon] \tag{B.7}$$

$$T_{D-EL4} = -4A_{rd}\omega_{Bn}\omega_{Ad} \sin \epsilon \tag{B.8}$$

$$T_{D-EL5} = 2A_{rd}\omega_{Bn}\omega_{Ad}tg^2 \epsilon \tag{B.9}$$

$$T_{D-EL6} = A_{rd}\omega_{Ad}^2 \left[ \frac{1}{\cos^2 \epsilon} - 2 \right] \tag{B.10}$$

$$T_{D-EL7} = (\dot{\omega}_{p_k} + \ddot{\eta})[A_{re} \sin \epsilon - A_{de} \cos \epsilon] \tag{B.11}$$

$$T_{D-EL8} = A_{rd}\omega_{Bn}^2 [-2 \sin^2 \epsilon + tg^2 \epsilon] \tag{B.12}$$

$$T_{D-EL9} = (A_d - A_r) \sin \epsilon \cos \epsilon + 2A_{rd}\omega_{Bn}^2 \tag{B.13}$$

$$T_{D-EL10} = (A_d - A_r)tg\epsilon[2\omega_{Ad}\omega_{Bn} \sin \epsilon - \omega_{Ad}^2 - \omega_{Bn}^2 \sin^2 \epsilon] \tag{B.14}$$

**References**

- [1] Masten MK. Inertially stabilized platform for optical imaging systems. *IEEE Control Syst Mag* 2008;28:47–64.
- [2] Analytic study of inside-out/coincident gimbal dynamics; final report, The Bendix corporation, Guidance System division; 1976.
- [3] Stokum LA, Carroll GR. Precision stabilized platform for shipborne electro-optical systems, 493. *SPIE*; 1984; 414–25.
- [4] Rue AK. precision stabilization systems. *IEEE Trans Aerosp Electron Syst* 1974;34–42 (AES-10).
- [5] Ekstrand B. Equations of motion for a two axes gimbal system. *IEEE Trans Aerosp Electron Syst* 2001;37:1083–91.
- [6] Daniel R. Mass properties factors in achieving stable imagery from a gimbal mounted camera, Published in *SPIE Airborne Intelligence, Surveillance, Reconnaissance (ISR) systems and applications V* 2008;6946.
- [7] Özgür, H, Aydan, E, Ismet, E. Proxy-based sliding mode stabilization of a two-axis gimbaled platform. In: *Proceedings of the world congress on engineering and computer science*. San Francisco. USA (WCECS). I; 2011.
- [8] Ravindra S. Modeling and simulation of the dynamics of a large size stabilized gimbal platform assembly. *Asian Int J Sci Technol Prod Manuf* 2008;1:111–9.
- [9] Khodadadi, H. Robust control and modeling a 2-DOF inertial stabilized platform. In: *International conference on electrical, control and computer engineering*. Pahang. Malaysia; 2011. p. 223–8.
- [10] Smith BJ, Schrenck WJ, Gass WB, Shtessel YB. Sliding mode control in a two axis gimbal system. In: *Proceedings of IEEE Aerospace Applications Conference*. 1999;5:457–70.
- [11] Willian, JB, Steven, PT. Optimal motion stabilization control of an electro-optical sight system. In: *Proceedings of SPIE Conference*. 1111; 1989; p. 116–20.
- [12] Bo L, Hullender D, DeRenzo M. Nonlinear induced disturbance rejection in inertial stabilization systems. *IEEE Trans* 1998;6:421–7.
- [13] Lin CM, Hsu CF, Mon YJ. Self-organizing fuzzy learning CLOS guidance law design. *IEEE Trans* 2003;39:1144–51.
- [14] Tam KK, Lee TH, Mamum A, Lee MW, Khoh CJ. composite control of a gyro mirror line of sight stabilization platform design and auto tuning. *ISA Trans* 2001;40:155–71.
- [15] Krishna Moorthy JAR, Marathe R, Sule VR. H $\infty$  control law for line-of-sight stabilization for mobile land vehicles. *Opt Eng* 2002;41:2935–44.
- [16] Li C, Jing W. Fuzzy PID controller for 2D differential geometric guidance and control problem. *IET Control Theory Appl* 2007;1:564–71.
- [17] Tong S, Li Y. Observer-based fuzzy adaptive control for strict-feedback nonlinear systems. *Fuzzy Sets Syst* 2009;160:1749–64.
- [18] Jamali N, Amlashi S. Design and implementation of fuzzy position control system for tracking applications and performance comparison with conventional PID. *IAES Int J Artif Intell (IJ-AI)* 2012;1:31–44.
- [19] Khuntia SR, Mohanty KB, Panda S, Ardil C. A comparative study of P-I, I-P, fuzzy and neuro-fuzzy controllers for speed control of DC motor drive, *World Academy of Science. Eng Technol* 2010;44:525–9.
- [20] Buckley J. Universal fuzzy controllers. *Autom J (IFAC)* 1992;28:1245–8.
- [21] Tong S, Li H. Fuzzy adaptive sliding-mode control for MIMO nonlinear systems. *IEEE Trans Fuzzy Syst* 2003;11:354–60.
- [22] Krishna Moorthy JAR, Marathe R, Hari B. Fuzzy controller for line of sight stabilization system. *Opt Eng* 2004;43:1394–400.
- [23] Tan KC, Lee TH, Khor EF. Design and real-time implementation of a multi-variable gyro-mirror line-of-sight stabilization platform. *Fuzzy Sets Syst* 2002;128:81–93.
- [24] AKARH M, TEMİZ İ. Motion controller design for the speed control of DC servo motor. *Int J Appl Math Inf* 2013;7:131–7.
- [25] Tanjung H, Sasongko PH, Suharyanto S. Performance analysis of hybrid PID-ANFIS for speed control of brushless DC motor base on identification model system. *Int J Computer Inf Technol* 2013;2:694–700.
- [26] Kennedy PJ, Kennedy RL. Direct versus indirect line of sight (LOS) stabilization. *IEEE Trans Control Syst Technol* 2003;11:3–15.
- [27] Hilkert JM. Inertially stabilized platform technology. *IEEE Control Syst Mag* 2008;28:26–46.
- [28] Yu S, Zhao Y. A new measurement method for unbalanced moments in a two-axis gimbaled seeker. *Chin J Aeronaut* 2010;23:117–22.
- [29] Tang KZ, Huang SN, Tan KK, Lee TH. Combined PID and adaptive nonlinear control for servo mechanical systems. *Mechatronics* 2004;14:701–14.
- [30] Malhotra R, Singh N, Singh Y. Design of embedded hybrid fuzzy-GA control strategy for speed control of DC motor: a servo control case study. *Int J Comput Appl* 2010;6:37–46.
- [31] Fujita, H, Sasaki, J. Torque control for DC servo motor using adaptive load torque compensation. In: *Proceedings of the ninth WSEAS international conference on System science and simulation in engineering*; 2010. p. 454–8.
- [32] Musaab, S. Design and simulation of servomechanism for rate gyro stabilized seeker. MSc thesis. MUT. Iran; 2010.
- [33] Ho-Pyeong L, Inn-Eark Y. Robust control design for a two-axis gimbaled stabilization system, *IEEEAC paper #1010*. version 2007;3:1–7.

- [34] Hilkert, JM, Hullender, DA., Adaptive control system techniques applied to inertial stabilization systems. In: Proceedings of SPIE Conference. 1304; 1990. 190–206.
- [35] Wahid N, Hassan N, Rahmat MF, Mansor S. Application of intelligent controller in feedback control loop for aircraft pitch control. Aust J Basic Appl Sci 2011;5:1065–74.
- [36] Karasakal O, Yesil E, Zelkaya MGU, Eksin I. Implementation of a new self-tuning fuzzy PID controller on PLC. Turk J Elec Engin 2005;13:277–86.
- [37] Qiao W, Mizumoto M. PID type fuzzy controller and parameters adaptive method. Fuzzy Sets Syst 1996;78:23–35.
- [38] Hu B, Mann GK, Gosine RG. A new methodology for analytical and optimal design of fuzzy PID controllers. IEEE Trans Fuzzy Syst 1999;7:521–39.
- [39] Rajani K, Mudi K, Pal R, Nikhil A. Robust self-tuning scheme for PI- and PD-type fuzzy controllers. IEEE Trans Fuzzy Syst 1999;7:2–16.